

Creep-fatigue failure of SAF 2205 and 316 stainless steels in Ar + 3%SO₂ environment at 700 °C

E. AGHION, C. A. MOLABA

Department of Mechanical Engineering, University of Natal, Durban 4001, South Africa

The creep-fatigue behaviour of SAF 2205 duplex stainless steel and 316 austenitic stainless steel was studied under a sulphur-containing environment of an Ar + 3%SO₂ atmosphere at 700 °C. The cyclic loading employed creep-tension and plastic compression following the creep-plasticity (cp)-mode of the strain-range partitioning life-prediction method. The results showed that a premature failure was obtained with both SAF 2205 and 316 stainless steels under the combination of creep-fatigue loading and an SO₂-bearing atmosphere. However, SAF 2205 was significantly more resistant than 316 as far as the number of cycles to failure and the sulphidizing attack at the external surface were concerned. In both materials, the creep-fatigue crack propagation was directly controlled by the environmental attack of the SO₂-containing environment at the region ahead of the crack tip.

1. Introduction

Recently, the use of stainless steels in areas such as gasification of coals and refinery application has been receiving increased attention due to the demanding conditions to which these materials are exposed during service [1, 2]. Two of the main conventional materials which are being offered for these conditions are SAF 2205 duplex stainless steel and 316 austenitic stainless steel. The service conditions in question combine the hostile high-temperature sulphidizing environment and a range of cyclic and monotonic loading conditions. The cyclic loading includes cyclic plasticity which arises as a result of start up and shut down procedures, together with the interspersed effects due to the "on-load" periods at high temperature.

One successful way to simulate those cyclic loading conditions is by applying the principles of the strain-range partition life-prediction technique [3]. This method involves the determination of the four basic life relationships resulting from the four possible combinations of plastic or creep strain range in the tensile or compressive halves of the fatigue cycle. These combinations are designated pp, pc, cp and cc, where the first letter indicates loading under tension and the second letter that under compression, while p stands for the plasticity mode and c for the creep mode of loading. This method is usually used for high-temperature mechanical testing in air and few studies have used this method for testing materials under different controlled environments [4, 5].

The present study aimed to evaluate the creep-fatigue behaviour of SAF 2205 and 316 stainless steels in a sulphidizing environment using the cp-mode of the strain-range partitioning method. This mode

of loading was selected because it was found to be one of the most damaging for many alloys [6]. For comparison purposes, tests were also carried out in an inert argon and air atmosphere.

2. Experimental procedure

The chemical composition of the materials used in the present work is shown in Table I. The fatigue specimens were machined from round bars and their dimensions and shape are shown in Fig. 1. The two collars on the specimen were cut in order to mount an extension measurement device (Linear Variable Differential Transducer, LVDT system) that measured the axial strain applied to the specimen.

The experimental apparatus for conducting creep-fatigue tests in a controlled atmosphere consisted of three principal parts: a gas mixing system, a standard MTS machine and a split-oven furnace, as schematically shown in Fig. 2. The gas mixing system was capable of producing any mixture of up to four different gases. This mixture was then delivered to the neck of the fatigue specimen which was enclosed in a shell attached loosely around the specimen. The mixture had a positive pressure aiming to eliminate the presence of air in the shell space. The MTS loading machine was equipped with hydraulic grips and had 100 kN capacity. The split furnace had a core diameter of 114 mm and was controlled by a three-zone control unit. The furnace was capable of reaching 1100 °C with an accuracy of ± 1 °C.

The creep-fatigue loading conditions were constant and consisted of creep tension and plastic compressions according to the cp-mode of the strain-range partitioning method at 700 °C. The strain range was

TABLE I Chemical composition of SAF 2205 and 316 stainless steel used in the present study

Alloy	Element (wt %)									
	Cr	Ni	Mo	Mn	Si	C	P	Cu	S	Fe
SAF 2205	21.19	5.75	2.59	1.44	0.49	0.022	0.021	0.14	0.005	Bal.
316	16.6	10.7	2.28	1.03	0.38	0.038	0.035	0.24	0.013	Bal.

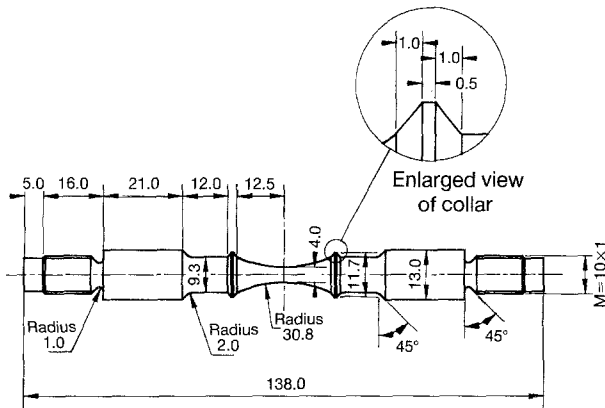


Figure 1 The creep-fatigue test specimen.

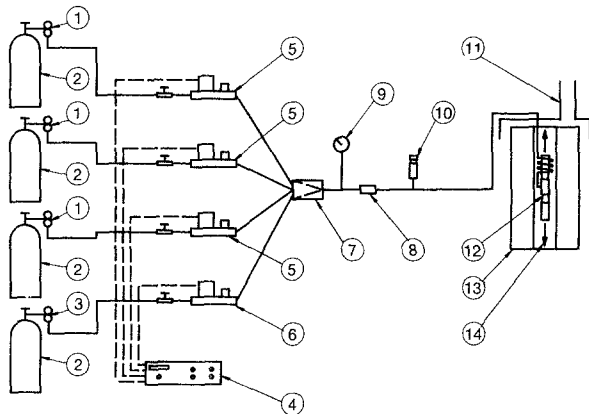


Figure 2 A schematic illustration of the experimental apparatus for conducting creep-fatigue tests in a controlled atmosphere. (1) Pressure regulator valve, (2) gas container, (3) pressure regulator valve (stainless steel) for highly corrosive gases, (4) gas mixing controller, (5) gas flow capacitor regulator, (6) gas flow capacity regulator (stainless steel) for highly corrosive gases, (7) conical gas mixing unit, (8) non-return valve, (9) pressure gauge, (10) pressure relief valve, (11) excess gas suction system, (12) cylindrical sleeve for hot gas, (13) split-oven furnace, (14) MTS loading system.

approximately 3.8×10^{-3} and the tensioning strain rate was $2.1 \times 10^{-4} \text{ s}^{-1}$ while compression was at a rate of $38 \times 10^{-4} \text{ s}^{-1}$. The SO_2 -containing environment was a mixture of $\text{Ar} + 3\% \text{SO}_2$, while air and pure argon were used as reference atmospheres.

A special corrosion chamber was designed and used to evaluate the environmental effect on unstressed specimens. The corrosion chamber was made up of an austenitic stainless steel and consisted of a device enabling disc specimens to be inserted into a ditch facing the environment. The pressure inside the corrosion chamber was again kept positive to eliminate air.

The disc specimens were also used for X-ray diffraction analysis in order to identify the various phases evolved under the different gas mixtures.

3. Results and discussion

The results showed clearly that a severe sulphidation attack occurred at the external surface of both SAF 2205 and 316 stainless steel under the combination of creep-fatigue loading and an $\text{Ar} + 3\% \text{SO}_2$ environment. This attack acted as the incubation and initiation stages of the fatigue crack propagation which developed perpendicular to the external loading direction. It should be noted that the sulphidation attack was significantly moderated with the unloaded disc specimens.

Typical changes in the sequence and shape of cyclic loading loops recorded during one of the creep-fatigue tests of 316 stainless steel in an $\text{Ar} + 3\% \text{SO}_2$ environment is shown in Fig. 3. Such shape changes included a continuous drop in the tensile stress amplitude of each consecutive loop and the decrease of the inelastic true strain. In terms of the crack opening displacement, the crack growth behaviour was represented by the bending of the upper part of the loop, which increases towards the final failure.

The fracture surface and the adjacent region after creep-fatigue failure of 316 stainless steel in an $\text{Ar} + 3\% \text{SO}_2$ environment is shown in Fig. 4a while the fracture surface in pure argon is shown in Fig. 4b. It is evident that a thick, cracked, sulphide layer was developed under the SO_2 -bearing atmosphere close to the fracture surface. A close-up view and chemical analysis of the fracture surface in $\text{Ar} + 3\% \text{SO}_2$ are shown in Fig. 5. This has revealed that the fracture surface was covered with sulphide and oxide phases and some secondary cracking was present. The fatigue crack propagation, including chemical analysis close to the crack tip, is shown in Fig. 6. The presence of nearly 7 wt % sulphur near the crack tip is probably an indication of a direct sulphidizing attack which may be combined with elemental sulphur being diffused from the environment to that region. In both cases the region ahead of the crack tip will become severely embrittled and hence an accelerated crack propagation is expected.

X-ray diffraction analysis spectrum of unloaded 316 disc specimen exposed to $\text{Ar} + 3\% \text{SO}_2$ at 700°C is shown in Fig. 7. Typical sulphide phases of the main alloying elements were evolved, namely Cr_3S_4 , Cr_2S_3 , NiS and Ni_3S_2 . This is due to the higher chemical affinity of these alloying elements to sulphur. The development of these brittle sulphide phase ahead of

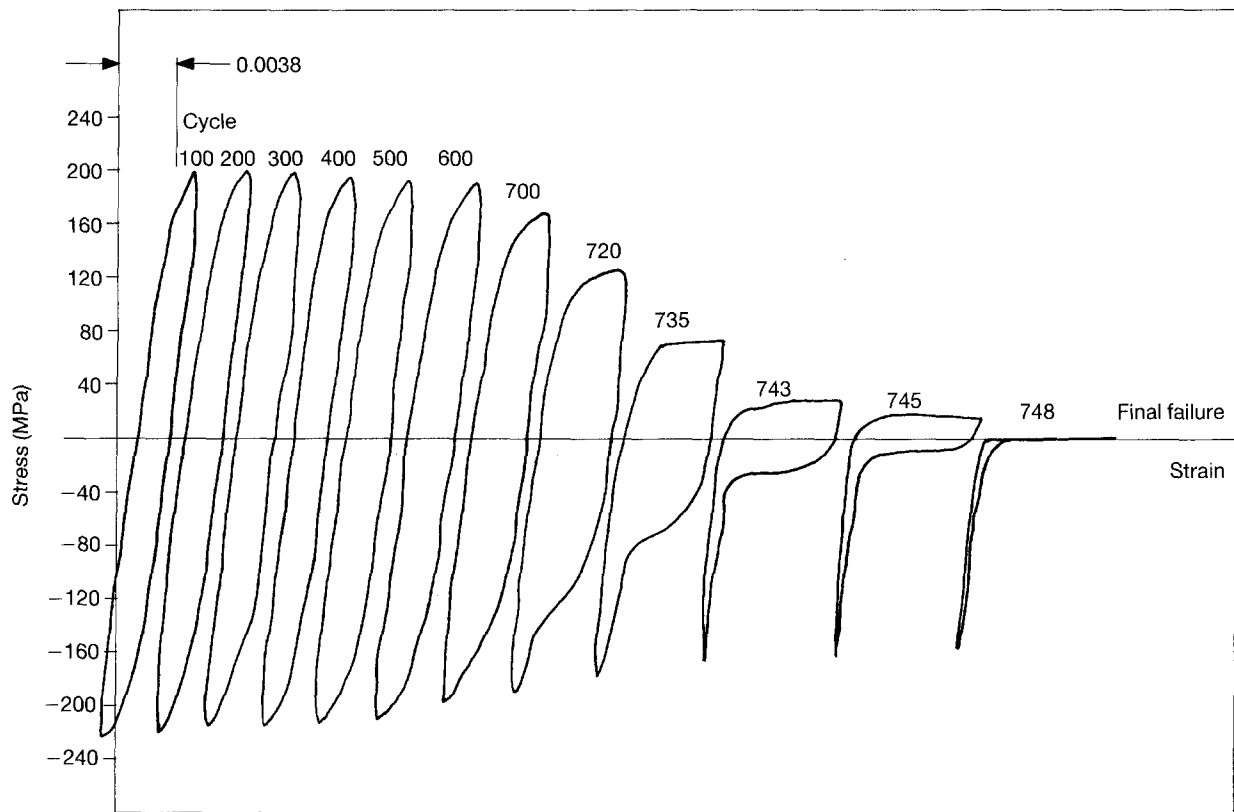


Figure 3 Typical hysteresis loops for cp-cycling, ($\Delta\epsilon = \pm 0.0038$) of 316 stainless steel in an Ar + 3%SO₂ environment at 700 °C.

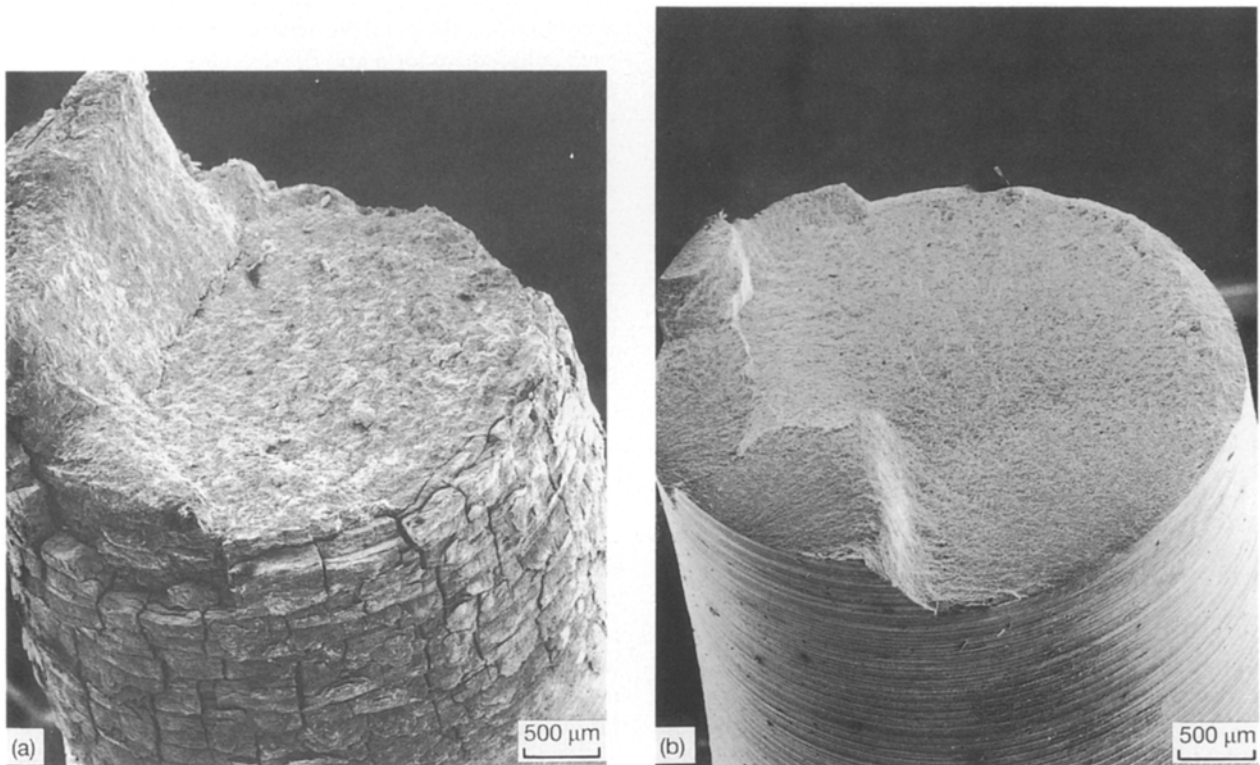


Figure 4 Fracture surface of 316 stainless steel obtained after creep-fatigue failure in (a) an Ar + 3%SO₂ environment, (b) a pure argon atmosphere.

the crack tip and the additional elemental sulphur diffusion to that region makes it more sensitive to cracking, and under the cyclic loading conditions, premature failure is inevitable.

The creep-fatigue failure mechanism of SAF 2205 duplex stainless steel in an Ar + 3%SO₂ environment was, in general, quite similar to that obtained with 316 stainless steel under the same conditions. However,

the sulphidizing effect of the environment was more moderate in SAF 2205. This resulted in a significant increase in the creep-fatigue life of SAF 2205, compared to that of 316 stainless steel.

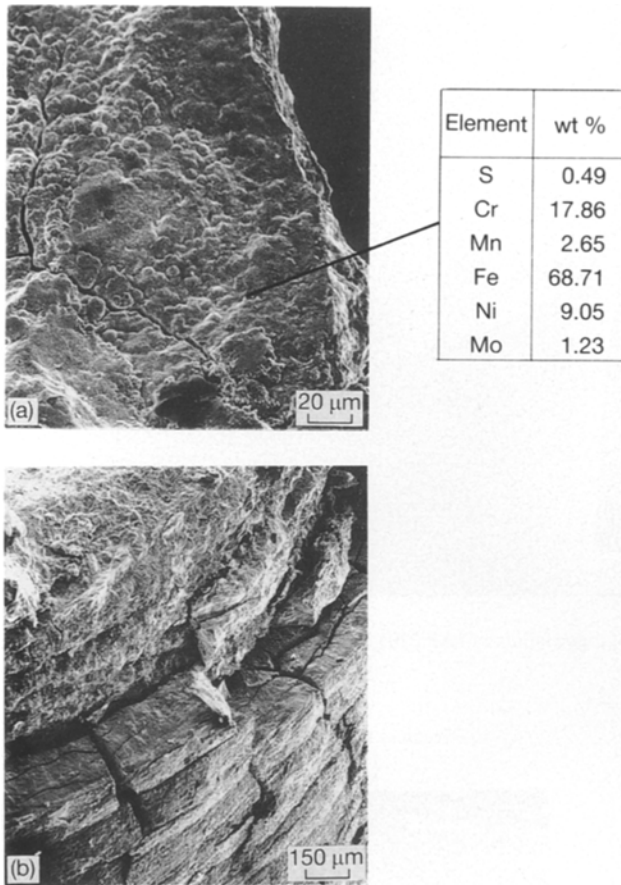


Figure 5 Close-up views of (a) the fracture surface and (b) the adjacent circumferential area of 316 stainless steel following creep-fatigue failure in an Ar + 3%SO₂ environment.

The fracture surface of SAF 2205 after creep-fatigue failure in an Ar + 3% SO₂ environment and in a pure argon atmosphere is shown in Fig. 8. It shows that part of the adjustment region close to the fracture surface in the Ar + 3%SO₂ atmosphere was covered with a cracked sulphide layer. A close-up view of the fracture surface under the sulphidizing atmosphere is shown in Fig. 9. The sulphur content in that region was 0.79 wt %, again indicating the presence of sulphide phases. Furthermore, it can be seen from Fig. 9b that the cracked sulphide layer has initiated cracks which could easily propagate through the alloy.

The microstructure at a longitudinal cross-section of the fracture surface of SAF 2205 in an Ar + 3%SO₂ atmosphere is shown in Fig. 10. The microstructure can be divided into two parts: the upper part was composed mainly of sulphide phases, while the lower part

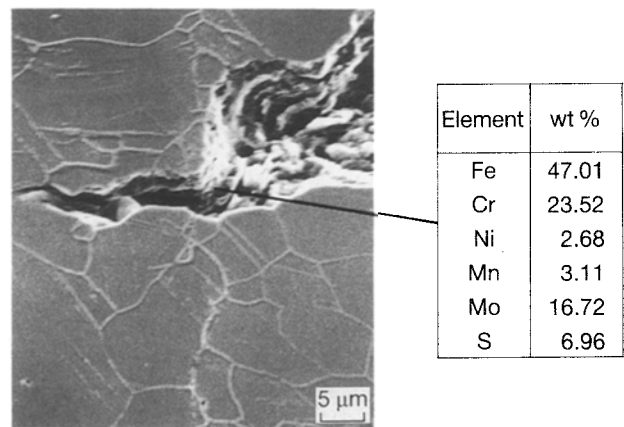


Figure 6 Microstructure and chemical composition of a propagating crack following a creep-fatigue failure of 316 alloy in an Ar + 3%SO₂ environment.

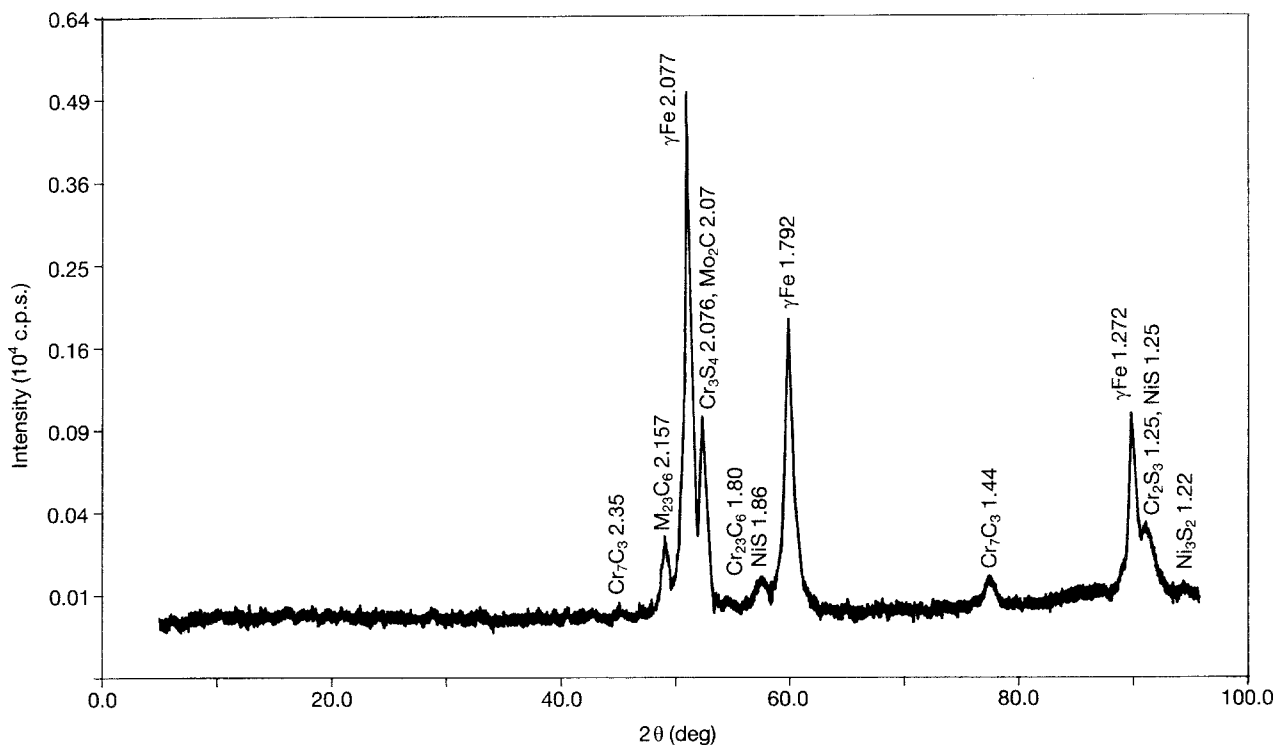


Figure 7 X-ray diffraction analysis spectrum of unloaded 316 disc specimen exposed to an Ar + 3%SO₂ environment at 700 °C, CoK_α radiation.

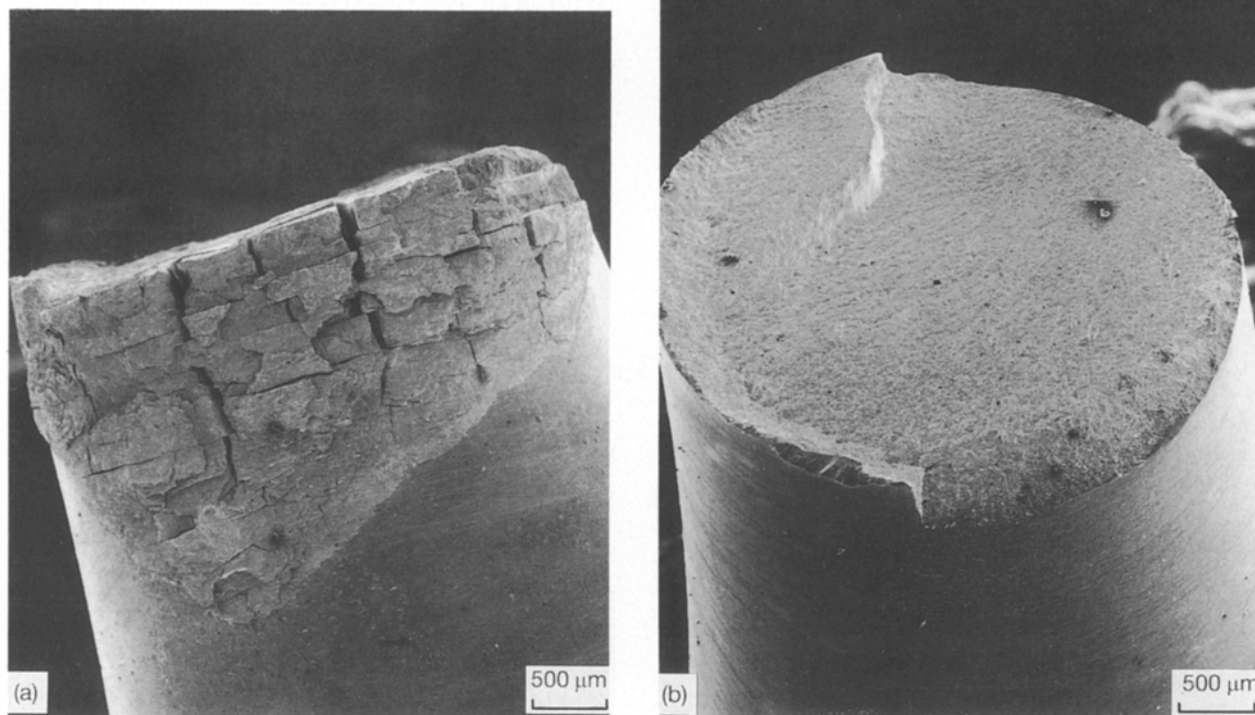


Figure 8 The fracture surfaces and the adjacent area obtained after creep-fatigue failure of SAF 2205 duplex stainless steel in (a) an Ar + 3% SO₂ environment, and (b) a pure argon atmosphere.

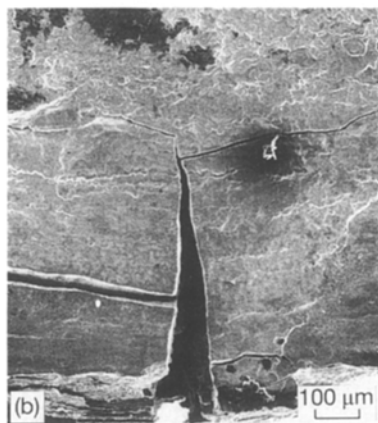
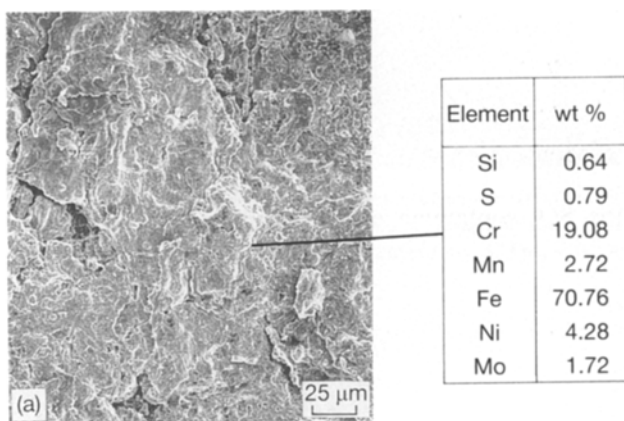


Figure 9 A close-up view of (a) the fracture surface and (b) the circumferential edge area of SAF 2205 duplex stainless steel after creep-fatigue failure in an Ar + 3%SO₂ atmosphere.

contained the regular duplex stainless steel microstructure. An interesting result of this was that the ferrite phase was preferentially attacked by the sulphidizing environment leaving behind “fingers” of austen-

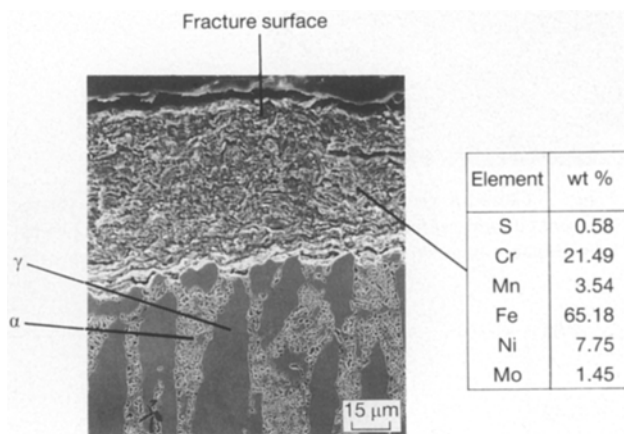


Figure 10 The microstructure at a longitudinal cross-section of the fracture surface of SAF 2205 alloy after creep-fatigue failure in an Ar + 3%SO₂ environment.

ite stuck in the rich mixture of sulphide phases. The apparently higher resistance of the austenite phase towards the sulphidizing environment is due to the fact that the ferrite phase has lower corrosion resistance in the tested conditions. As a result, the sulphidizing attack and the interaction by elemental sulphur will be preferentially concentrated on the ferrite phase. Following this explanation, it is believed that the ferrite phase provides a temporary cathodic protection to the austenite phase which at a later stage will also be directly attacked by the sulphidizing atmosphere once the ferrite has corroded away.

An X-ray diffraction analysis spectrum of unloaded SAF 2205 disc exposed to an Ar + 3%SO₂ environment is shown in Fig. 11. Again, the typical sulphide phases of the main alloying elements Cr₂S₃, NiS and

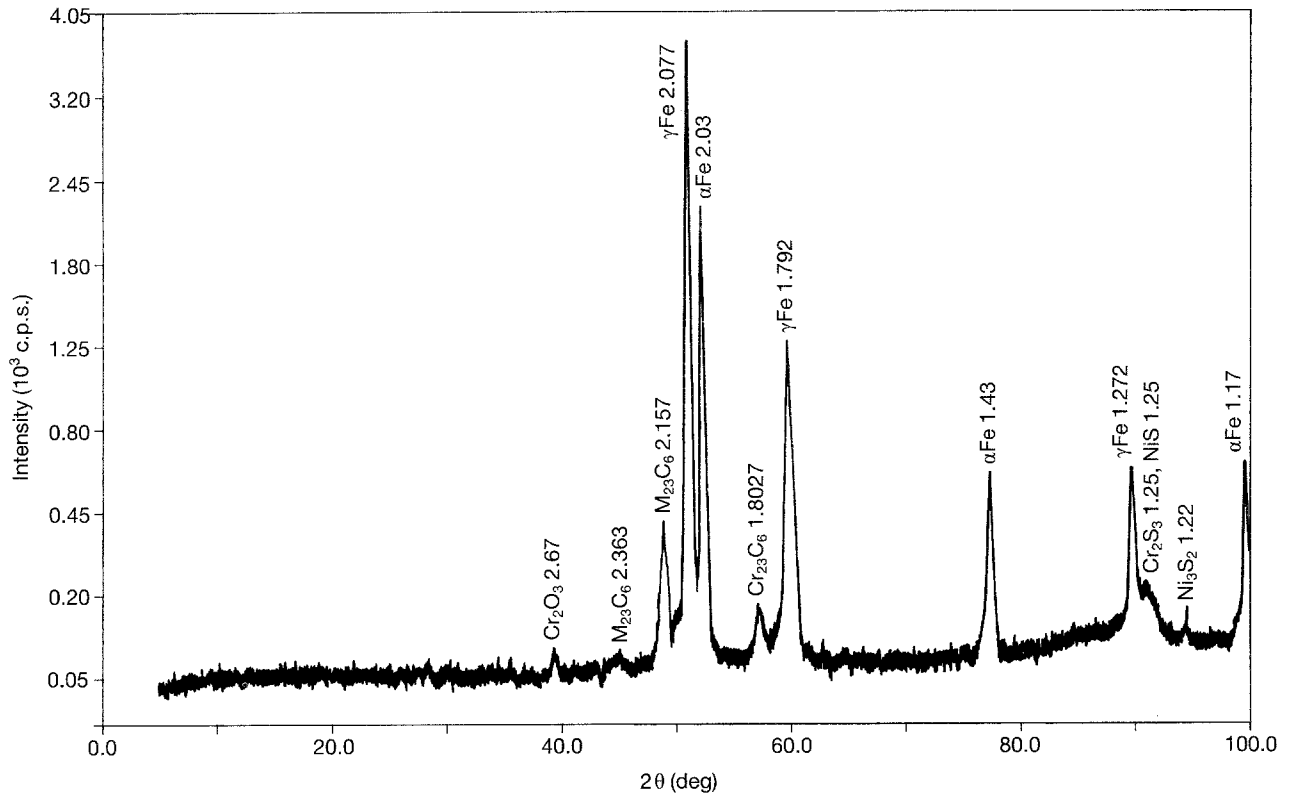


Figure 11 X-ray diffraction spectrum obtained from an unloaded SAF 2205 stainless steel disc specimen exposed to an Ar + 3%SO₂ atmosphere at 700 °C, CoK_α radiation.

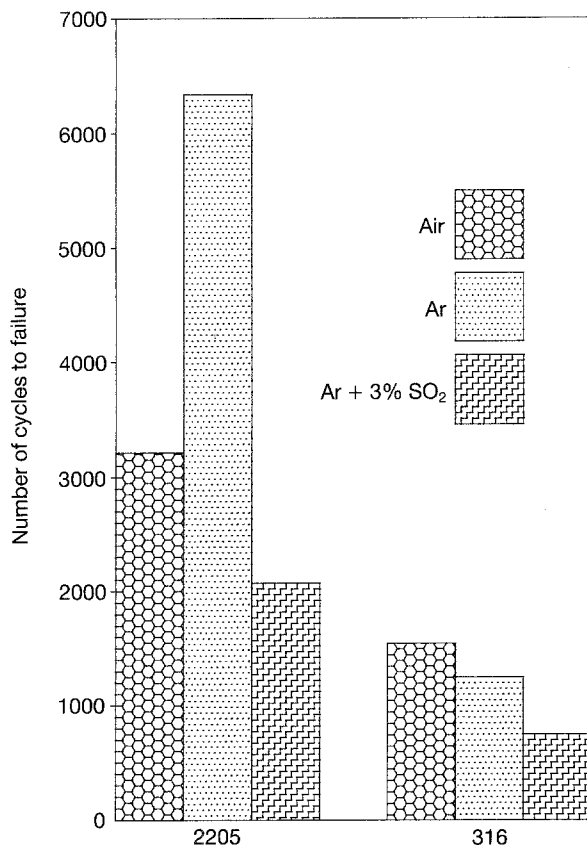


Figure 12 The environmental effect on creep-fatigue life of SAF 2205 and 316 stainless steel at 700 °C (cp-cycling $\Delta\epsilon = \pm 0.0038$).

Ni₃S₂ were present, and it is likely that their effect on the creep-fatigue crack-growth behaviour was similar to that obtained with the 316 stainless steel.

It is clear that in the SO₂-containing environment, a premature failure was obtained with both SAF 2205

and 316 stainless steel as shown in Fig. 12 which represents average results of several tests (each result was an average of at least four measurements) carried out for each alloy under the specific loading and environment conditions. However, it is also evident from Fig. 12 that the creep-fatigue life of SAF 2205 in the SO₂-containing environment was higher by at least a factor of two compared to the life obtained with the 316 stainless steel. This genuine effect of the SO₂-containing environment on the creep-fatigue life of the two alloys may be explained through the difference in the chromium content. This is due to the fact that the chromium has a higher corrosion resistance in an SO₂ environment compared to the resistance of the other main elements comprising the two stainless steels, namely iron and nickel [7]. As a result, it would be expected that SAF 2205, which has a higher chromium content than 316 stainless steel, will be more resistant to the SO₂-containing atmosphere and hence will have a relatively prolonged creep-fatigue life.

Finally, it should be noted that the results obtained in the present study support the assertion made by Barteri *et al.* [8]. They indicate that SAF 2205 duplex stainless steel may represent an optimized technical-economic choice in many high-temperature sulphur-bearing atmospheres when an intrinsically corrosion-resistant stainless steel with high mechanical properties is required.

4. Conclusions

1. The combination of creep-fatigue loading and an Ar + 3%SO₂ environment have resulted in a severe sulphidation attack at the external surface, followed

by a premature failure of both SAF 2205 and 316 stainless steel.

2. The sulphidation attack at the surface acted as the incubation and initiation stages for fatigue crack propagation.

3. SAF 2205 was significantly more resistant than 316 stainless steel in the Ar + 3%SO₂ environment. This was manifested in a marked difference in the number of cycles to failure.

4. The direct sulphidizing attack and the elemental sulphur diffusion at a region ahead of the propagating crack tip in both SAF 2205 and 316 stainless steel causes an embrittlement of that region and hence directly controlled the nature of the crack-growth behaviour.

Acknowledgement

The authors thank Middelburg Steel and Alloys S.A. for supporting this research project.

References

1. D. A. MILLER, R. H. PRIEST and E. G. ELLISON, *High temp. Mater Proc.* **6** (3/4) (1984) 156.

2. J. F. NORTON, F. G. HODGE and G. Y. LAI, in "International Conference Proceedings on High Temperature Materials for Power Engineering 1990", Liege, Belgium 24–27 September 1990, edited by E. Bachelet, R. Brunetaud, D. Coutouradis, P. Esslinger, J. Ewald, I. Kvernes, Y. Lindblom D. B. Meadowcroft, V. Regis, R. B. Scarlin, K. Schneider and R. Singer (Kluwer Academic, 1990) p. 167.
3. A. BERKOVITS, S. NADIV and G. SHALEV, in "Proceedings of the International Conference on Fatigue, Corrosion Cracking, Fracture Mechanics and Failure Analysis" (ASM, Salt Lake City, UT, 1985) p. 399.
4. E. AGHION, M. BAMBERGER and A. BERKOVITS, *Mater. Sci. Eng.* **26** (1991) 1873.
5. E. AGHION, M. BAMBERGER and A. BERKOVITS, *Mater. Sci. Eng.* **A147** (1991) 181.
6. S. S. MANSON and G. R. HALFORD, in 25th ISR, "Complexities of high temperature metal fatigue", Israeli Conference on Aeronautics and Astronautics, Haifa (1983) p. 33.
7. M. G. FONTANA and N. D. GREENE, "Corrosion Engineering" (McGraw-Hill, 1987) p. 376.
8. M. BARTERI, F. NACIA, A. TAMBA and G. MONTAGNA, *Corros. Sci.* **27** (1987) 1239.

Received 23 September 1992

and accepted 27 September 1993